Electronic Supplementary Material (ESI) for Nanoscale.
This journal is © The Royal Society of Chemistry 2020

Supporting Information

Electroreduction of nitrogen to ammonia on nanoporous gold

Haibin Ma,[‡,a] Zhiwen Chen,[‡,a] and Zhili Wang*[a]

[a] Key Laboratory of Automobile Materials, Ministry of Education, and School of Materials Science and Engineering, Jilin University, Changchun 130022, China

*E-mail: zhiliwang@jlu.edu.cn

‡These authors contributed equally to this work.

Experimental Procedures

Chemicals

Hydrogen peroxide (H_2O_2, 30%), nitric acid (HNO_3, 65.0%~68.0%), sodium hydroxide (NaOH, 96.0%), salicylic acid ($C_7H_6O_3$, 99.5%), ammonium chloride (NH_4Cl, 99.5%), sodium citrate dehydrate ($C_6H_5Na_3O_7 \cdot 2H_2O$, 99.0%) were purchased from Sinopharm Chemical Reagent Co., China. Hydrochloric acid (HCl, 35.0%~38.0%) and ethanol (C_2H_5OH, 99.7%) were obtained from Beijing Chemical Works, China. Hydrazine monohydrate ($N_2H_4 \cdot H_2O$, 99.0%), iron phthalocyanine ($C_{32}H_{16}FeN_8$, 96.0%) and dimethyl sulfoxide-d_6 (DMSO-d_6, deuterium for 99.9%) were obtained from Alfa Aesar, USA. Sodium nitroferricyanide dehydrate ($C_5FeN_6Na_2O \cdot 2H_2O$, 99.0%) and D_2O (99.9%) were obtained from Sigma-Aldrich, USA. Sodium hypochlorite solution (NaClO, available Cl 4.0%) was obtained from Shanghai MACKLIN Chemical Works, China. P-dimethylaminobenzaldehyde (PDAB, $C_9H_{11}NO$, 99%) was obtained from Adamas-beta Chemical Co., Switzerland. Nitrogen (N_2, high purity 99.999%) and argon (Ar, high purity 99.999%) were purchased from Ju'yang gas Co., China. $^{15}N_2$ (enrichment of > 99% atom ^{15}N) was obtained from Shanghai Research Institute of Chemical Industry Co., China. All chemical were commercial and used without further purification. Ultrapure water (18.2 MΩ cm) was used in all experiments.

Preparation of NPG catalysts

The NPG catalysts were prepared using an electrochemical dealloying method in a standard three-electrode cell with a Pt gauze as the counter electrode and a Ag/AgCl

electrode as the reference electrode. The $Au_{35}Ag_{65}$ leaf (3 cm × 3 cm) was used as the work electrode and dealloyed in 0.1 M HNO_3 solution by using an electrochemical workstation with a dealloying potential of 1.307 V versus RHE. The obtained NPG samples were carefully rinsed with ultrapure water to remove residual acid and impurity ions. All electrochemical potentials were determined with respect to RHE using the equation (Eq. 1):

$$E(RHE) = 0.198 + 0.059\,pH + E(Ag/AgCl) \quad (1)$$

Microstructural and chemical characterization

The morphological and lattice structural information of the NPG samples were investigated with field emission SEM (FEI Nano430) and TEM (JEM-2100F) combined with an EDS. XPS was performed using Physical Electronics 5400 ESCA photoelectron spectrometer.

Electrochemical measurements

Before NRR test, the Nafion 115 membranes were heat-treated in 5.0 wt% H_2O_2 solution, 0.5 M H_2SO_4 solution, and ultrapure water for 1 h, respectively.[1] Electrochemical measurements were performed using a gas-tight two-compartment electrochemical cell separated by a piece of Nafion 115 membrane at room temperature. The Pt gauze and Ag/AgCl electrode were used as counter electrode and reference electrode, respectively. The work electrode was prepared by placing the NPG film onto glassy carbon electrode (0.07 cm^{-2}). The linear sweep voltammetry was conducted at a scan rate of 20 mV/s. The electrocatalytic performance of NPG

catalyst for NRR was evaluated using controlled potential electrolysis in 0.1 M HCl aqueous solution for 2 h at room temperature (~25 ^{o}C). The electrolyte was presaturated with N_2 by N_2 gas bubbling for at least 30 min prior to each measurement. During the measurement, the electrolyte was continuously bubbled with N_2 at a flow rate of 10 sccm.

Ammonia quantification

The produced NH_3 was quantitatively determined by the indophenol blue method.[2] Typically, 2.0 mL of the sample solution was first pipetted from the electrochemical reaction vessel. Afterwards, 2.0 mL of NaOH solution (1.0 M) containing $C_7H_6O_3$ (5.0 wt%) and $C_6H_5Na_3O_7$ (5.0 wt%), 1.0 mL of NaClO solution (0.05 M), and 0.2 mL of $C_5FeN_6Na_2O$ solution (1.0 wt%) were added into the above solution. After 2 h, the absorption spectra of the resulting solution were acquired with an UV-vis spectrophotometer (Varian Cary 50). The obtained indophenol blue was measured by absorbance at λ = 656 nm. In order to quantify the produced NH_3, the calibration curve was built using standard NH_4Cl solutions in the presence of 0.1 M HCl. The measurements with the background solutions (no NH_3) were performed for all experiments, and the background peak was subtracted from the measured peaks of NRR experiments to calculate the NH_3 concentrations and the Faradaic efficiencies.

Hydrazine quantification

The produced N_2H_4 was determined by the method of Watt and Chrisp.[3] The color reagent was obtained by mixing 4.99 g of PDAB with 20 mL of concentrated

HCl and 200.0 mL of C_2H_5OH. And then 5.0 mL of the electrolyte solution was taken out and mixed with 5.0 mL of the above color reagent. After 15 min, the absorption spectra of the resulting solution were acquired using a UV-vis spectrophotometer. The N_2H_4 solution with known concentrations in 0.1 M HCl were used as calibration standard, and the absorbance at λ = 458 nm was used to plot the calibration curve.

Calculation of the Faradaic efficiency and NH_3 yield rate

The Faradaic efficiency was calculated from the charge consumed for NH_3 production and total charge passed through the electrode during the electrolysis (Eq. 2):[4]

$$\text{Faradaic efficiency} = [3F \times (C_{NH3,N2} - C_{NH3,Ar}) \times V)]/17Q \quad (2)$$

The NH_3 yield rate was calculated using the following equation (Eq. 3):[4]

$$\text{NH}_3 \text{ yield rate} = [(C_{NH3,N2} - C_{NH3,Ar}) \times V)]/(t \times m) \quad (3)$$

Where F is the Faradaic constant (96485 C mol^{-1}), C_{NH3} is the measured NH_3 concentration (μg mL^{-1}), V is the volume of the electrolyte, Q is the total charge passed through the electrode, t is the electrolysis time (2 h), and m is the metal mass of the catalyst (0.018 mg).

Calculation method for the overpotential of NRR

The NRR occurs at 0.06 V versus RHE theoretically, therefore the overpotential of NRR can be calculated via the following formula (Eq. 4):

$$\text{Overpotential} = 0.06 \text{ V} - E \text{ (V, versus RHE)} \quad (4)$$

$^{15}N_2$ Isotope Labeling Experiments

An isotopic labeling experiment using $^{15}N_2$ (enrichment of > 99% atom ^{15}N) as the feed gas was conducted to elucidate the activity origin of NPG. Before the electrochemical reduction procedure, the electrolyte was purged with high purity Ar to remove the ^{14}N in the electrolyte and saturated with $^{15}N_2$ for 30 min with the flow rate of 10 sccm. After ^{15}NRR for 2 h at −0.1 V versus RHE in 0.1 M HCl solution, the obtained $^{15}NH_4^+$ electrolyte was determined by 1H nuclear magnetic resonance (NMR, Bruker, Avance Ⅲ 600 MHz). To prepare the NMR sample, 20 mL of electrolyte after NRR was concentrated to ~ 1 mL, then 30 μL of 100 ppm dimethyl sulfoxide-d_6 (DMSO-d_6) and 70 μL D_2O was added in the solution. Similarly, the amount of $^{14}NH_4^+$ was determined by this method when $^{14}N_2$ (99.999%) was used as the feed gas. All NMR measurements were carried out with water suppression and 4000 scans.

DFT calculation methods

All DFT calculations were performed in the Dmol3 code with the spin polarization.[5] The generalized gradient approximation (GGA) with Perdew-Burke-Ernzerhof functional (PBE) was applied to describe the exchange-correlation effects.[6] The relativistic effects were implemented by DFT semicore pseudopotentials core treatment with the basis set of double numerical plus polarization (DNP).[7] For geometrical optimization, the convergence criteria of energy change, gradient, and displacement were 1.0×10^{-5} hartree, 2.0×10^{-3} hartree $Å^{-1}$, and 5.0×10^{-3} Å, respectively. TS method for DFT-D correction was used to accurately describe the van der Waals forces.[8] The vacuum gap set to be about 15 Å, which should lead to negligible interactions between the system and their mirror images. The

computational hydrogen electrode (CHE) model was used for calculating the reaction processes.[9] Thus, the reaction free energy (ΔG) was determined by $\Delta G = \Delta E + \Delta ZPE - T\Delta S + \Delta G_U$, where ΔE, ΔZPE, T, ΔS, and ΔG_U indicated the reaction energy, zero point energy, temperature, change of entropy, and free energy contribution due to the electrode potential (U), respectively.

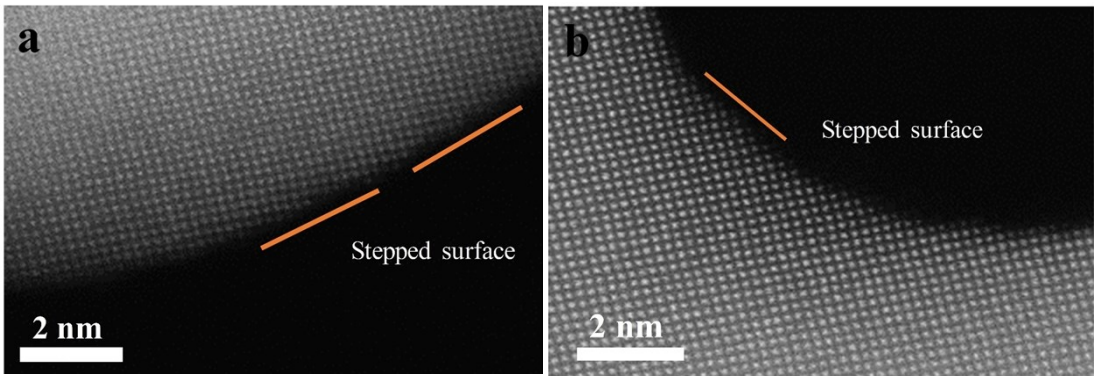

Fig. S1. (a, b) Atomic resolution HAADF-STEM image of curved surfaces of Au ligaments with abundant atomic steps and kinks.

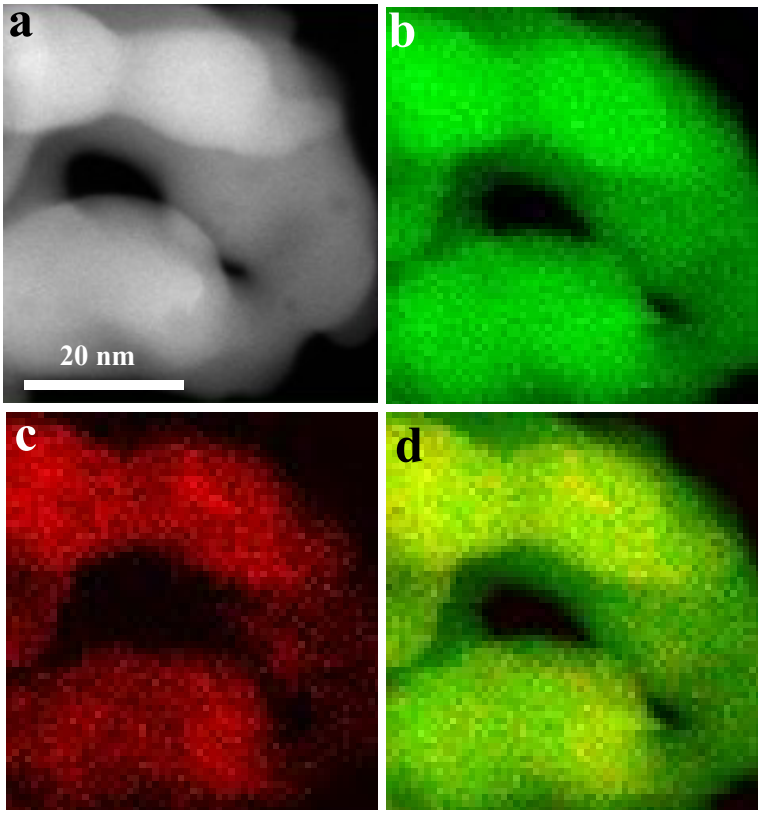

Fig. S2. (a) STEM images and corresponding EDS elemental mappings of (b) Au-Lα (gree), (c) Ag-Lα (red), and (d) mixed-color images of NPG.

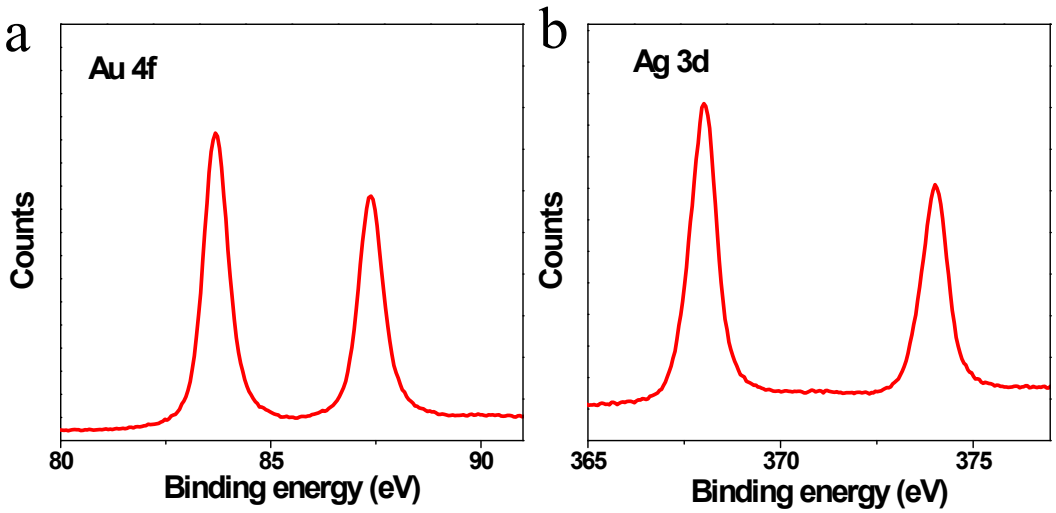

Fig. S3. High resolution XPS characterization of (a) Au 4f and (b) Ag 3d peaks of NPG.

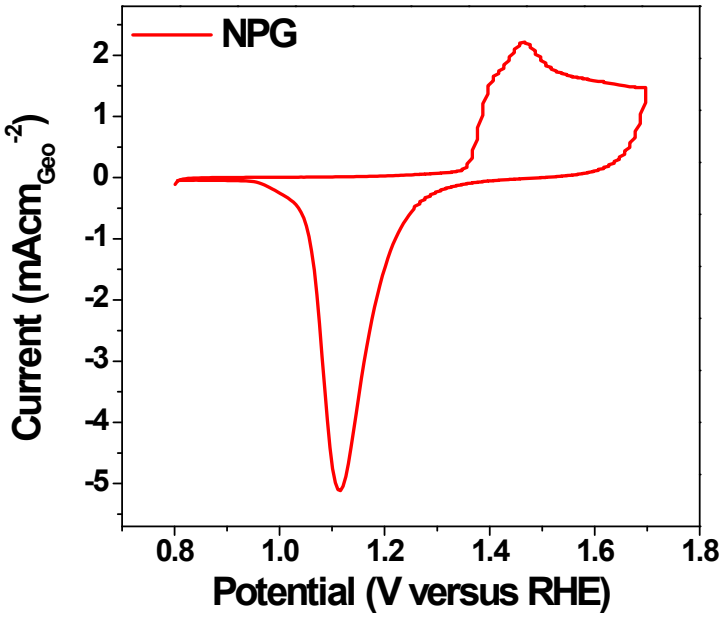

Fig. S4. CV curve of the NPG sample (dealloyed at 1.307 V versus RHE) recorded in 0.05 M H_2SO_4 solution with a scan rate of 50 mV s^{-1}.

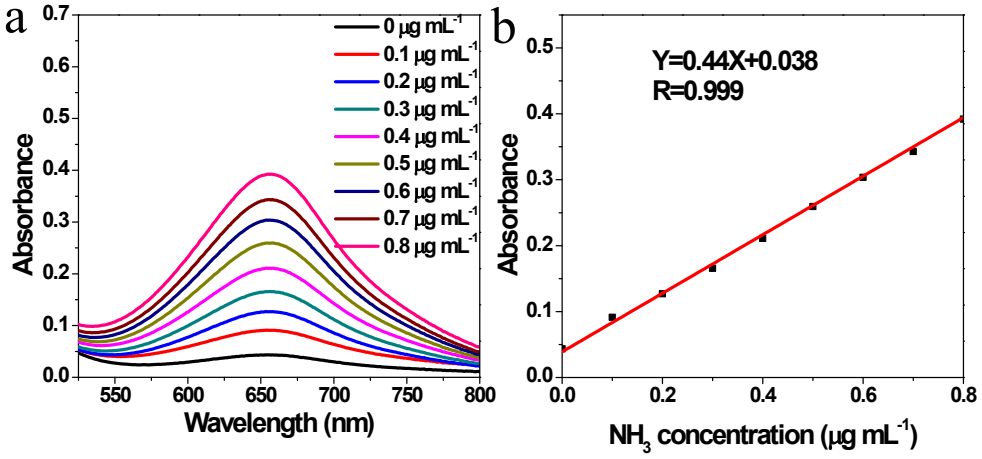

Fig. S5. (a) The UV-vis absorption spectra and (b) the corresponding calibration curve for the colorimetric NH_3 assay in 0.1 M HCl solution.

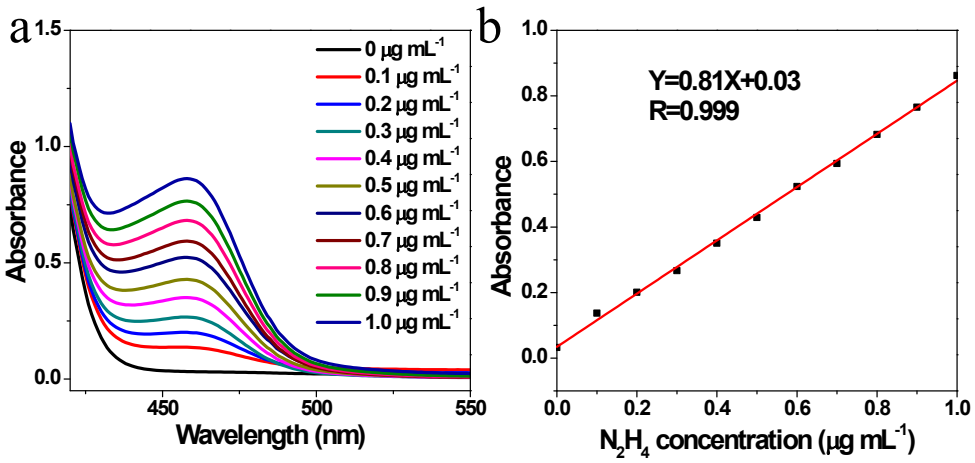

Fig. S6. (a) The UV-vis absorption spectra and (b) the corresponding calibration curve for the colorimetric N_2H_4 assay in 0.1 M HCl solution.

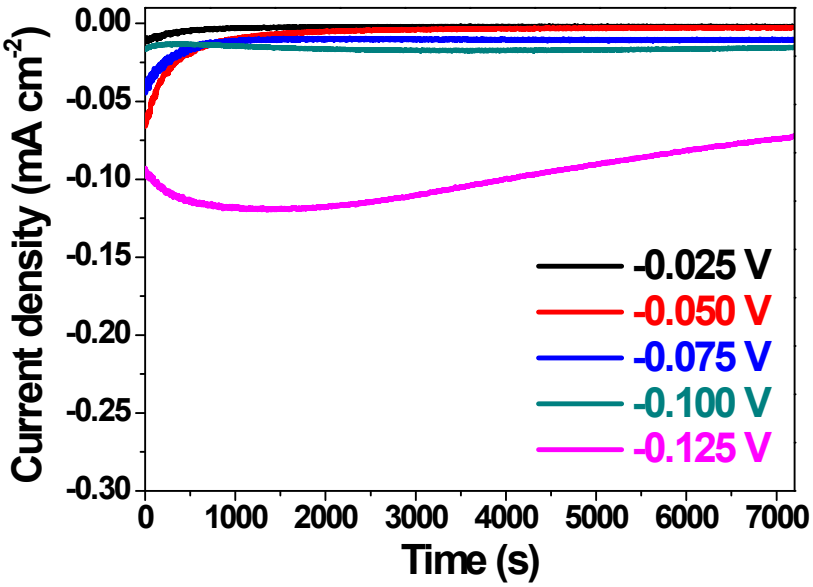

Fig. S7. Chronoamperometric curves of the NPG catalyst in N_2-saturated 0.1 M HCl solution at various potentials.

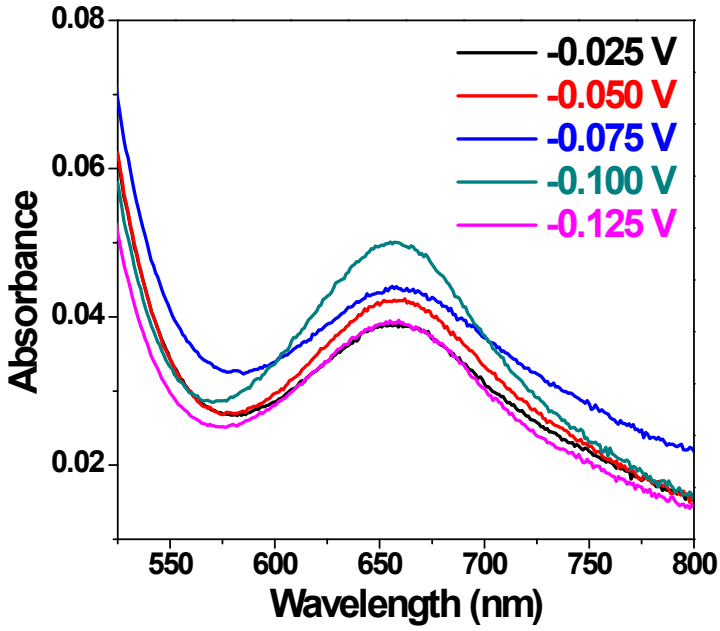

Fig. S8. UV-vis absorption spectra of the 0.1 M HCl electrolytes stained with indophenol indicator after electrolysis at different potentials for 2 h with the NPG catalyst.

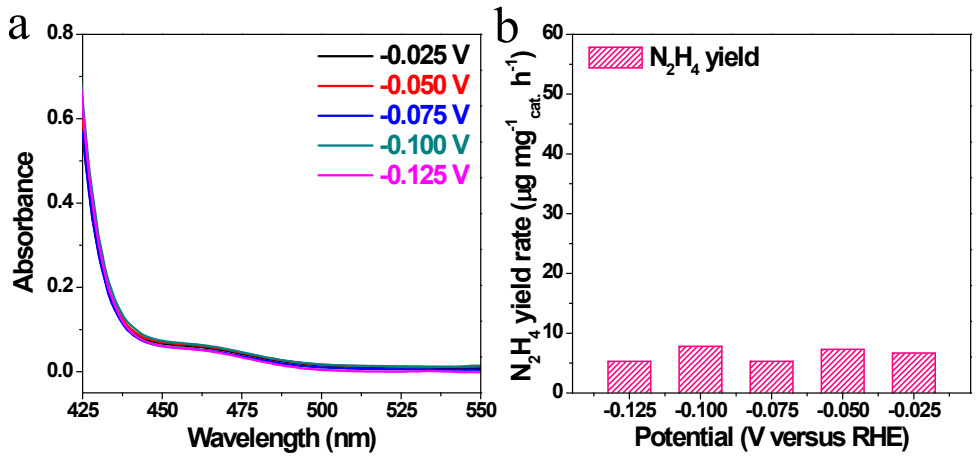

Fig. S9. (a) UV-vis absorption spectra and (b) the corresponding N_2H_4 yield rates of the NPG catalyst in N_2 saturated 0.1 M HCl solution at different potentials.

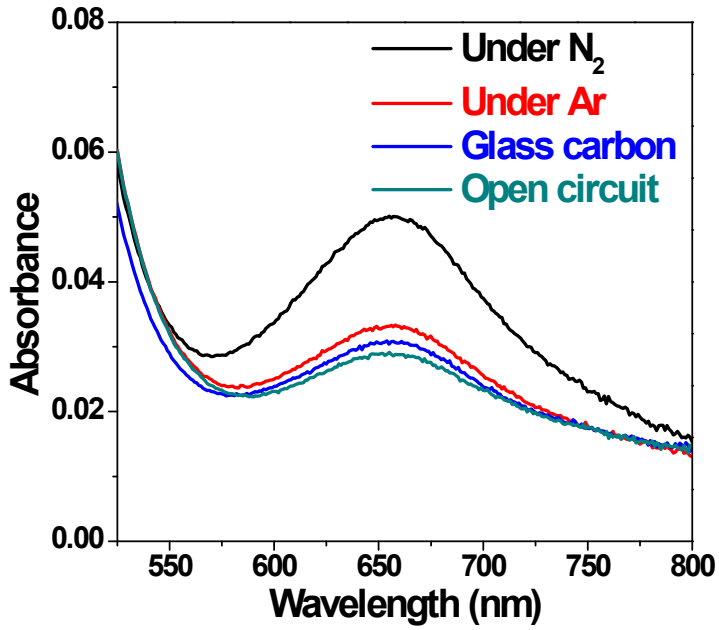

Fig. S10. UV-vis absorption spectra of the electrolytes stained with indophenol indicator after electrolysis at −0.10 V versus RHE for 2 h under various conditions.

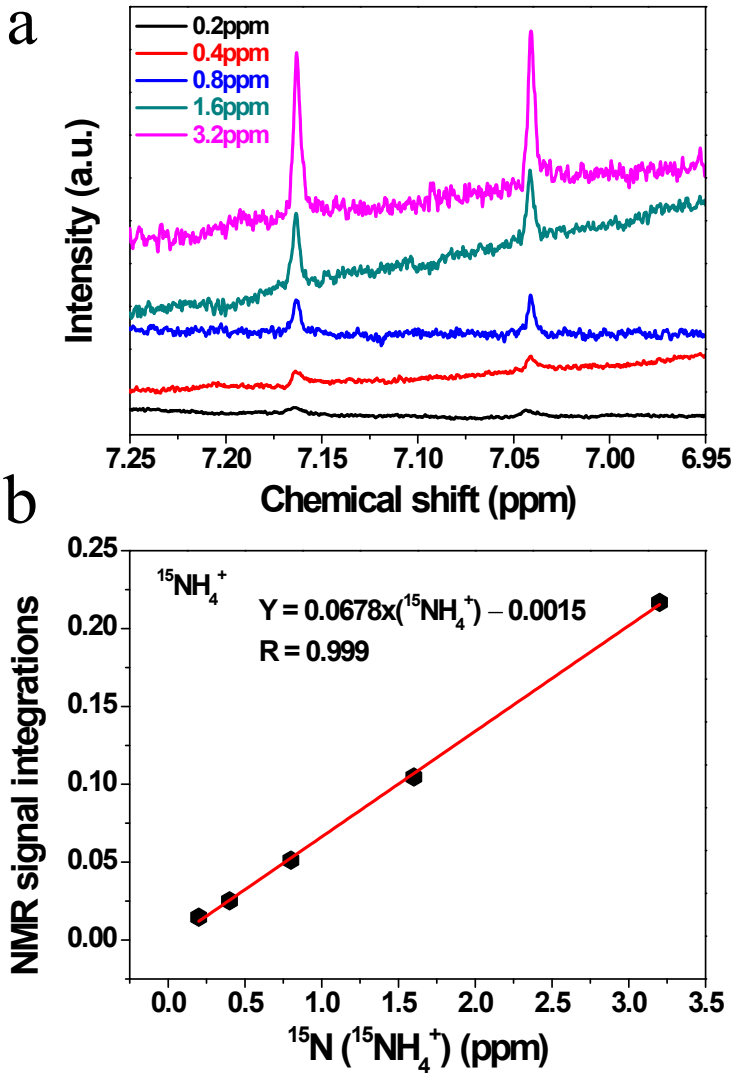

Fig. S11. (a) The ^{1}H-NMR spectra of $^{15}NH_4^+$ standard with different concentrations, (b) the corresponding calibration curve of $^{15}NH_4^+$ concentration against relative signal integration based on the ^{1}H-NMR spectra. Based on this calibration curve, the $^{15}NH_3$ yield rate at -0.10 V versus RHE is calculated to be 42.6 μg h^{-1} $mg^{-1}_{cat.}$, which is consistent with the result of $^{14}N_2$ reduction experiment.

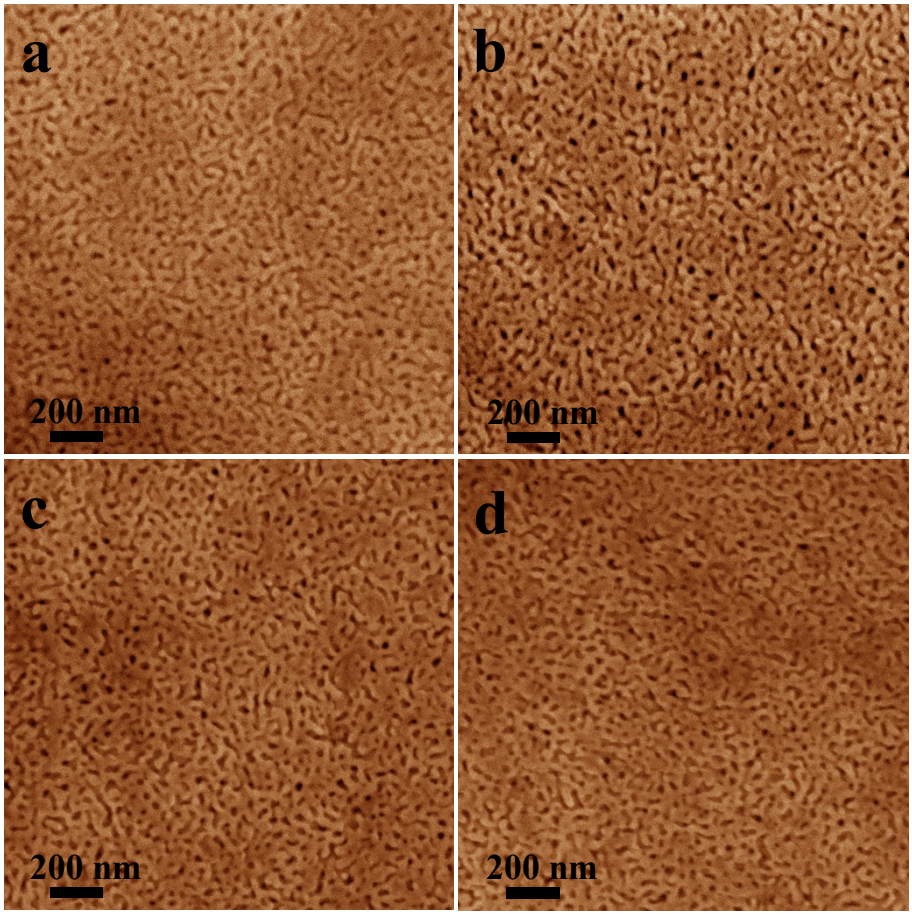

Fig. S12. SEM images of NPG samples prepared at the dealloying potential of (a) 1.257 V, (b) 1.287 V, (c) 1.327 V and (d) 1.357 V.

.

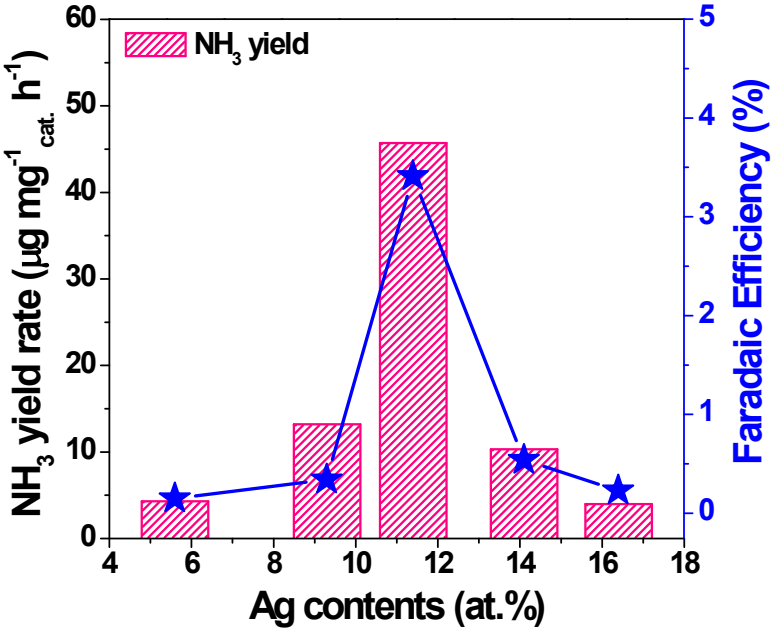

Fig. S13. NH_3 yield rates and Faradaic efficiencies of NPG catalysts with different Ag contents.

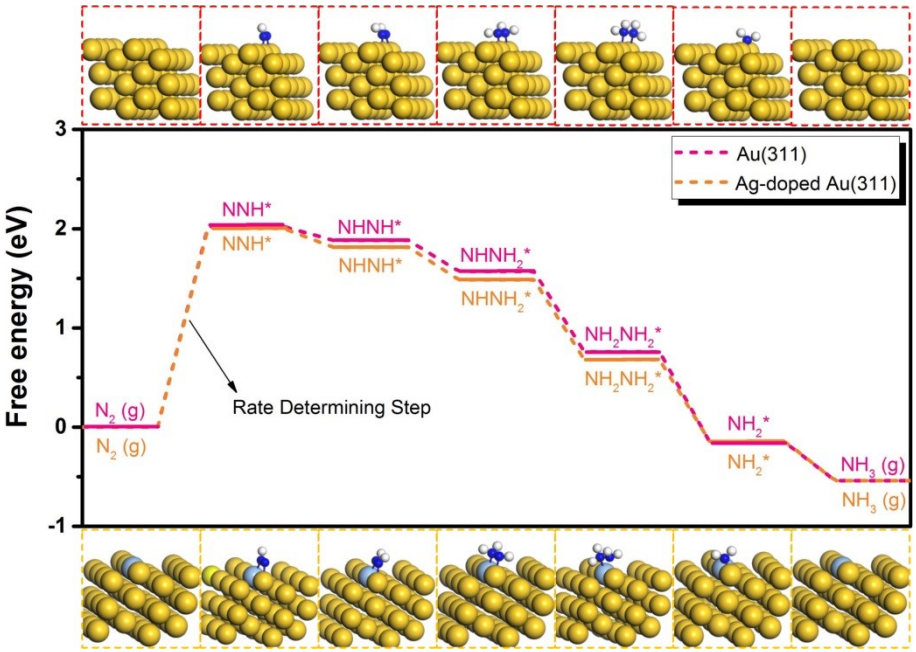

Fig. S14. Free energy diagrams and corresponding geometric structures of intermediates of NRR on Au (311) and Ag-doped Au (311).

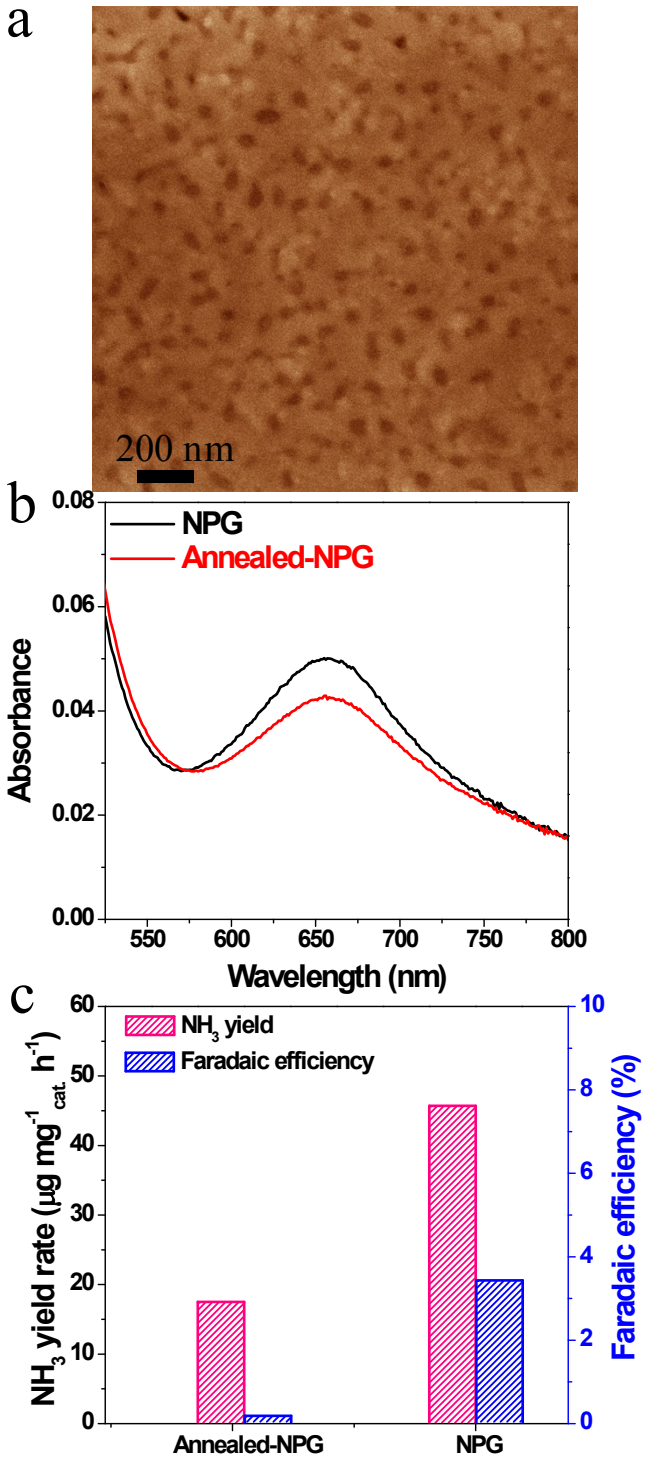

Fig. S15. (a) SEM image of the annealed NPG with the ligament sizes of ~72.4 nm. (b) UV-vis absorption spectra and (c) corresponding NH_3 yield rates and Faradaic efficiencies of annealed NPG and as-prepared NPG.

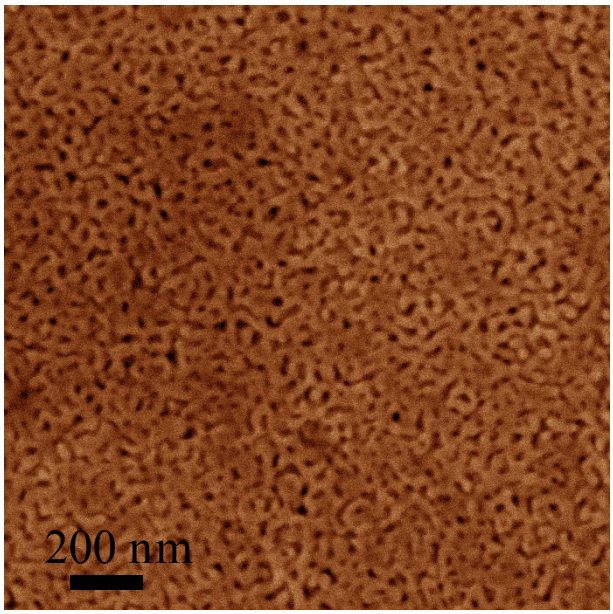

Fig. S16. SEM image of NPG catalyst after stability test.

Table S1. Ag contents in NPG samples prepared at different dealloyed potentials.

Sample	Dealloying Potential (V versus RHE)	Ag content (%)
1	1.257	16.4
2	1.287	14.1
3	1.307	11.4
4	1.327	9.3
5	1.357	5.6

Table S2. Comparison of NRR electrocatalytic activity of NPG catalyst and other electrocatalysts at room temperature and ambient condition.

Catalyst	Electrolyte	NH_3 yield rate ($\mu g\ mg^{-1}_{cat.}\ h^{-1}$)	Faradaic efficiency (%)	Overpotential (mV)	Ref.
NPG	0.1 M HCl	45.7 (11.4 $\mu g\ cm^{-2}\ h^{-1}$)	3.41	160	This work
Au/TiO_2	0.1 M HCl	21.4	8.1	260	10
Au/CeO_X-RGO	0.1 M HCl	8.3	10.1	260	11
Au HNCs	0.5 M $LiClO_4$	3.74 $\mu g\ cm^{-2}\ h^{-1}$	35.9	460	12
THH Au NRs	0.1 M KOH	1.648 $\mu g\ cm^{-2}\ h^{-1}$	4.02	260	13
Ag-Au/ZIF	THF solution	6.12 $\mu g\ m^{-2}\ h^{-1}$	18	2960	14
SA-Ru/N-C	0.05 M H_2SO_4	120.9	29.6	260	15
PdRu TPs	0.1 M KOH	37.23	1.85	260	16
Fe-N/C hybrid	0.1 M KOH	34.83	9.28	260	17
FL-BP NSs/CF	0.01 M HCl	31.37	5.07	660	18
SA-Mo/NPC	0.1 M KOH	34.0	14.6	360	19
MoS_2	0.1 M Na_2SO_4	29.28	8.34	460	20
Cr_2O_3	0.1 M Na_2SO_4	25.3	6.78	960	21
$Bi_4V_2O_{11}/CeO_2$	PH=1 HCl	23.21	10.16	260	22
MoC/C	0.5 M Li_2SO_4	11.3	7.8	360	23
Pd/C	0.1 M PBS	4.5	8.2	56	1
PEBCD/C	0.5 M Li_2SO_4	1.58 $\mu g\ cm^{-2}\ h^{-1}$	2.85	560	24
Fe_2O_3/CNT	$KHCO_3$	0.22 $\mu g\ cm^{-2}\ h^{-1}$	<0.05	260	25
Fe/Fe_3O_4	0.1 M PBS	0.19 $\mu g\ cm^{-2}\ h^{-1}$	8.29	360	26

Notes and references

1 J. Wang, L. Yu, L. Hu, G. Chen, H. Xin and X. Feng, *Nat. Commun.,* 2018, **9**, 1795.

2 P. L. Searle, *Analyst,* 1984, **109**, 549-568.

3 G. W. Watt and J. D. Chrisp, *Anal. Chem.,* 1952, **24**, 2006-2008.

4 L. F. Greenlee, J. N. Renner and S. L. Foster, *ACS Catal.* 2018, **8**, 7820-7827.

5 B. Delley, *J. Chem. Phys.,* 2000, **113**, 7756-7764.

6 J. P. Perdew, K. Burke and M. Ernzerhof, *Phys. Rev. Lett.,* 1996, **77**, 3865.

7 B. Delley, *Phys. Rev. B.,* 2002, **66**, 155125.

8 A. Tkatchenko and M. Scheffler, *Phys. Rev. Lett.,* 2009, **102**, 073005.

9 J. H. Montoya, C. Tsai, A. Vojvodic and J. K. Norskov, *ChemSusChem.,* 2015, **8**, 2180-2186.

10 M. M. Shi, D. Bao, B. R. Wulan, Y. H. Li, Y. F. Zhang, J. M. Yan and Q. Jiang, *Adv. Mater.,* 2017, **29**, 1606550.

11 S. J. Li, D. Bao, M. M. Shi, B. R. Wulan, J. M. Yan and Q. Jiang, *Adv. Mater.,* 2017, **29**, 1700001.

12 M. Nazemi and M. A. El-Sayed, *J. Phys. Chem. Lett.,* 2018, **9**, 5160-5166.

13 D. Bao, Q. Zhang, F. L. Meng, H. X. Zhong, M. M. Shi, Y. Zhang, J. M. Yan, Q. Jiang and X. B. Zhang, *Adv. Mater.,* 2017, **29**, 1604799.

14 H. K. Lee, C. S. L. Koh, Y. H. Lee, C. Liu, I. Y. Phang, X. Han, C. K. Tsung and X. Y. Ling, *Sci. Adv.,* 2018, **4**, eaar3208.

15 Z. Geng, Y. Liu, X. Kong, P. Li, K. Li, Z. Liu, J. Du, M. Shu, R. Si and J. Zeng, *Adv. Mater.,* 2018, **30**, 1803498.

16 H. Wang, Y. Li, C. Li, K. Deng, Z. Wang, Y. Xu, X. Li, H. Xue and L. Wang, *J.*

Mater. Chem. A., 2019, **7**, 801-805.

17 Y. Wang, X. Cui, J. Zhao, G. Jia, L. Gu, Q. Zhang, L. Meng, Z. Shi, L. Zheng, C. Wang, Z. Zhang and W. Zheng, *ACS. Catal.,* 2019, **9**, 336-344.

18 L. Zhang, L. X. Ding, G. F. Chen, X. Yang and H. Wang, *Angew. Chem. Int. Ed.,* 2019, **131**, 1-6.

19 L. Han, X. Liu, J. Chen, R. Lin, H. Liu, F. Lu, S. Bak, Z. Liang, S. Zhao, E. Stavitski, J. Luo, R. R. Adzic and H. Xin, *Angew. Chem. Int. Ed.,* 2019, **58**, 2321-2325.

20 X. Li, T. Li, Y. Ma, Q. Wei, W. Qiu, H. Guo, X. Shi, P. Zhang, A. M. Asiri, L. Chen, B. Tang and X. Sun, *Adv. Energy Mater.,* 2018, **8**, 1801357.

21 Y. Zhang W. Qiu, Y. Ma, Y. Luo, Z. Tian, G. Cui, F. Xie, L. Chen, T. Li and X. Sun, *ACS Catal.,* 2018, **8**, 8540-8544.

22 C. Lv, C. Yan, G. Chen, Y. Ding, J. Sun, Y. Zhou and G. Yu, *Angew. Chem. Int. Ed.,* 2018, **130**, 6181-6184.

23 H. Cheng, L. X. Ding, G. F. Chen, L. Zhang, J. Xue and H. Wang, *Adv. Mater.,* 2018, **30**, 1803694.

24 G. F. Chen, X. Cao, S. Wu, L. Zeng, X. Ding, M. Zhu and H. Wang, *J. Am. Chem. Soc.,* 2017, **139**, 9771-9774.

25 S. Chen, S. Perathoner, C. Ampelli, C. Mebrahtu, D. Su and G. Centi, *ACS Sustainable Chem. Eng.,* 2017, **5**, 7393-7400.

26 L. Hu, A. Khaniya, J. Wang, G. Chen, W. E. Kaden and X. Feng, *ACS Catal.* 2018, **8**, 9312-9319.